Economic, Exergy, Environmental (3E) Analysis of Methanol Production from Shale Gas

Weida Li[a], Yu Zhuang[b], Linlin Liu[a], Lei Zhang[a], Jian Du[a,*]

[a]Institute of Process Systems Engineering, School of Chemical Engineering, Dalian University of Technology, 116024 Dalian, China
[b]School of Energy and Power Engineering, Dalian University of Technology, 116024 Dalian, China
 dujian@dlut.edu.cn

Compared with direct utilisation as fuel, the downstream processing of shale gas shows great potential in economic competitiveness, in which methanol is a particularly important product. This study simulates a technical route for producing methanol from shale gas, which is evaluated from the points of economic, exergy and environment. The economic target is estimated by purchased cost curves, while exergy analysis demonstrates the distribution of exergy destruction. A hybrid LCI (Life cycle inventory) model is established to assess pollutant emissions by sources. The results show that methane reforming features the highest capital cost, while methanol synthesis requires the highest operating cost. The reaction systems account for 73.3 % of total exergy destruction. Electricity consumption dominates the environmental impacts of the whole process.

1. Introduction

According to the reports by the US Energy Information Administration (EIA), technically recoverable shale gas takes up 31.8 % of global natural gas resources (EIA, 2013). Recently, the large-scale exploitation of shale gas reduces the price of natural gas. In addition to using as an energy source, the downstream processing of shale gas is a promising option (Siirola, 2014).

As a vital feedstock widely applied in chemical synthesis, methanol is a particularly significant product among the various chemicals produced from shale gas. The process of methanol production includes gas purification, methane reforming and methanol synthesis. Purification removes the inherent contaminants in raw gas. The purified gas is sent to the cryogenic section to separate methane and heavier hydrocarbons (Rahimi et al., 2017). Methane is then fed to a reforming reactor to produce syngas. Partial oxidation is employed in this study, which is reported to have an advantage in economic over other reforming alternatives (Julián-Durán et al., 2014). Finally, the syngas is delivered to synthesise methanol.

An increasing interest has been shown in the downstream processing of shale gas in recent years. Ehlinger et al. (2014) simulated an integrated process for producing methanol and implemented a sensitivity analysis to optimise return on investment. However, this study is limited to the target in economic. The environmental and energy performances were not taken into account. Moreover, the synthesis reaction is modelled from the point of view of thermodynamics but ignored the aspect of kinetics. Julián-Durán et al. (2014) compared four reforming technologies and carried out an economic and environmental assessment. The carbon emissions were analysed, whereas the distribution of environmental impact from each subprocess was not considered. Ortiz-Espinoza et al. (2017) investigated the production of ethylene from shale gas, which was a complicated process with massive demands for energy and work. However, the exergy efficiency was not evaluated.

In this study, a 3E (economic, exergy and environmental) analysis of producing methanol from shale gas is conducted. The processes of purification and methane reforming are simulated by Aspen Plus v8.6 (Aspen Technology Inc., 2014), while the module of methanol synthesis is established in Visual C++ program, on the basis of a rigorous reaction model. The economic performance is estimated on the basis of the purchased cost curves, and the distribution of exergy destruction is acquired by exergy analysis. A hybrid LCI model is established to classify the pollutant emissions by processes and sources. The methods developed in this study provide a reference for process optimisation and environmental protection.

2. Process description

2.1 Shale gas purification

Purification is a crucial process to eliminate the impurities in raw gas. Table 1 presents a typical composition of raw shale gas. In general, the first step of purification is sweetening process which removes acid gases. Since studied previously (Li et al., 2018), sweetening treatment would not be considered in this work.

Table 1: Composition of shale gas (Li et al., 2018)

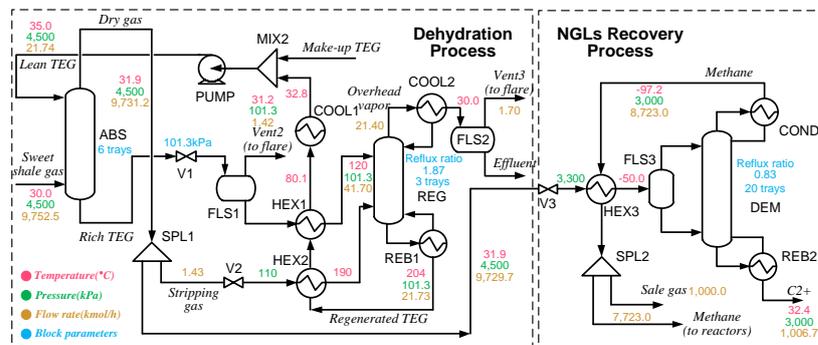| Components	Concentration/vol.%
CH_4	84.58
C_2H_6	6.51
C_3H_8	1.90
$n-C_4H_{10}$	0.74
$i-C_4H_{10}$	0.55
$n-C_5H_{12}$	0.13
$i-C_5H_{12}$	0.17
N_2	2.75
CO_2	0.82
H_2O	1.64

Figure 1: Schematic diagram of shale gas purification

The shale gas via sweetening treatment contains a certain amount of water. A TEG (Triethylene glycol)-based dehydration process is developed to remove water, as shown in Figure 1. The water content in the dry gas decreases to 74 ppm after absorption in the 6-tray absorber, while the rich glycol solvent is sent to the regenerator of 3 trays where water is distilled out. In order to enhance solvent regeneration, a small share of dry gas is split as stripping gas. The purity of regenerated TEG is 99.05 wt%. The remaining dry gas enters the followed NGLs (Natural gas liquids) recovery system. Methane is separated in the demethanizer (20 trays). The cryogenic methane enters HEX3 to precool the inlet gas. Then, 11.5 % of the purified methane is divided and sent to methanol production, while the rest is transported in pipelines for sale. The property method for sweetening process is PSRK, while the thermodynamic model adopted in NGLs recovery is Peng-Robinson.

2.2 Methanol production

Figure 2 shows the flowsheet of producing methanol from methane, which could be divided into two parts, methane reforming and methanol synthesis. The approach of methane reforming investigated in this work is partial oxidation (POX). The main reaction occurring in the POX reactor is

$$CH_4 + 0.5O_2 \rightarrow CO + 2H_2 \qquad \Delta H^o_{298K} = -35.99 kJ/mol \qquad (1)$$

The reactor operates at 1,300 °C and 2.8 MPa (Julián-Durán et al., 2014). So the inlet methane needs to be preheated. As for the inlet oxygen (0.4 MPa), a two-stage compression and heat exchange with methane are executed, in view of compression ratio and temperature in industrial practice. Based on the simulation results, the H_2:CO ratio of the syngas is 1.84 after oxidation reaction. The high-temperature syngas is sent to the waste heat boiler to produce high-pressure steam and chilled to 500 °C. Then, it is cooled to condense and separate the water generated from the side reactions. The syngas is subsequently compressed to 7.5 MPa and delivered to the methanol synthesis reactor. The property method for POX process is Peng-Robinson.
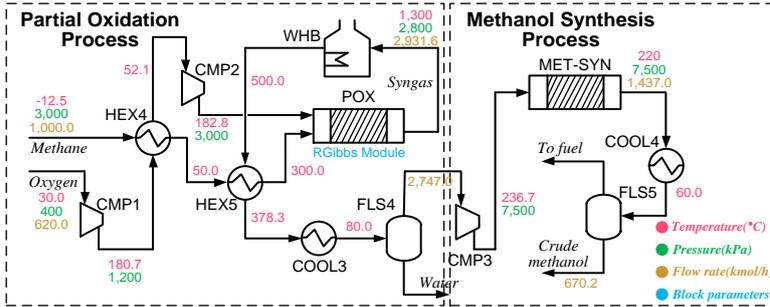
Figure 2: Schematic diagram of methanol production

The mechanism of methanol synthesis is recognised as the combination of CO and H_2 for a long period of time. However, in recent years, the majority of researchers are inclined to advocate the pathways of water gas shift reaction Eq.(2) and CO_2 hydrogenation Eq.(3) (Vanden Bussche and Froment, 1996)

$$CO + H_2O \rightarrow CO_2 + H_2 \qquad \Delta H^o_{298K} = \text{-41.17 kJ/mol} \tag{2}$$

$$CO_2 + 3H_2 \rightarrow CH_3OH + H_2O \qquad \Delta H^o_{298K} = \text{-49.24 kJ/mol} \tag{3}$$

In this work, the mechanism and kinetics developed by Vanden Bussche and Froment (1996) are employed to calculate the yield of methanol in Visual C++ program. The reactions occur in an isothermal tubular reactor catalysed by Cu/ZnO/Al$_2$O$_3$, operating at 220 °C and 7.5 MPa. The reactor has 20,000 tubes of 2.4 m and a diameter of 0.016 m. The usage of the catalyst is 0.348 kg per tube. The capacity of methanol production is 500 metric tons per day.

3. The methodology of 3E analysis

3.1 Economic evaluation

Total annual cost (TAC) of the overall process is evaluated, involving two parts, the annual capital cost (ACC) and the annual operating cost (AOC). The operating cost is defined as the annual average of fixed capital investment (Towler and Sinnott, 2013)

$$ACC = 1.68 \cdot ISBL \cdot j(1+j)^k / ((1+j)^k - 1) \tag{4}$$

where j and k are interest rate (15 %) and plant life time (15 y). ISBL is inside battery limit including the costs of major process equipment, which is calculated by purchased cost curves

$$ISBL = \sum_{i=1} F_i \cdot C_i = \sum_{i=1} F_i \cdot (A_i + B_i \cdot S_i^{n_i}) \tag{5}$$

where S is size parameter, while constants A, B, n and Hand's Factor F are determined by equipment type. Note that these parameters are all on the U.S. Gulf Coast basis in January 2010. So the Chemical Engineering Plant Cost Index (CEPCI) is used to update the costs of equipment at current prices

$$ISBL_{2017} = CEPCI_{2017} / CEPCI_{2010} \cdot ISBL_{2010} \tag{6}$$

The CEPCI in the year 2017 and January 2010 are 567.5 and 532.9.

Table 2: Unit price for items in AOC calculation

Process	Unit	Price
Steam (high pressure)	$\cdot$kJ^{-1}	1.42×10^{-5}
Steam (low pressure)	$\cdot$kJ^{-1}	8.68×10^{-6}
Fired heat	$\cdot$kJ^{-1}	4.25×10^{-6}
Cooling water	$\cdot$kJ^{-1}	6.83×10^{-7}
Refrigerant	$\cdot$kJ^{-1}	2.14×10^{-6}
Electricity	$\cdot$kW$^{-1}\cdot$h^{-1}	0.07
Shale gas loss	$\cdot$Nm^{-3}	0.3

On the other hand, the operating cost includes the expenses of utilities, electricity, fired heat and shale gas loss. Different grades of steam are utilised as hot utilities to provide heat sources in TEG regenerator and demethanizer. Cooling water is employed as a cold utility. In addition, ethylene refrigerant is another cold utility which is applied to the separation of methane. Electricity is mainly consumed to drive the compressors and pumps. The fired heat is adopted to provide energy for the POX reactor. Ultimately, the loss of shale gas which occurs during dehydration is also taken into account. The AOC is calculated on the basis of the usage for each item, the price of which is listed in Table 2, assuming an annual operating duration of 8,000 h.

3.2 Exergy analysis

The simulation results present the energy requirement of the whole flowsheet but fail to evaluate the work loss in irreversible processes. In this work, exergy analysis is conducted to calculate the exergy loss in each unit operation and provide guidance for improving thermodynamic performance. The exergy for a process stream includes physical exergy and chemical exergy. The former one reflects the distinctions in pressure and temperature between stream and ambience

$$Ex^{PH} = (h - h_0) - T_0(s - s_0) \tag{7}$$

where Ex, h and s are unit exergy, unit enthalpy and unit entropy. The subscript '0' represents the item of ambience.

Chemical exergy denotes the distinctions in chemical composition between stream and ambience

$$Ex^{CH} = \sum_i x_i Ex_i^{CH} + RT_0 \sum_i x_i \ln x_i \tag{8}$$

The ambient model developed by Kameyama et al. (1982) is employed as a standard state for chemical exergy. Under steady-state conditions, exergy destruction is calculated as:

$$Ex_d = \sum Ex_{inlet} - \sum Ex_{outlet} \tag{9}$$

3.3 Environmental assessment

In this work, a hybrid LCI model is proposed for a thorough assessment of environmental performances for the life cycle of shale gas to methanol. The environmental impacts of the whole process are divided into embodied emissions and process emissions. The former refers to the pollutants related to the upstream manufacture of equipment and raw materials, which are estimated by the input-output model (Chang et al., 2014). The process emissions are supplemented to evaluate the impacts during process operation.

Since upstream manufacture is complex processes where various industrial sectors involved, an input-output LCI model is employed to achieve the linkages between environmental impacts and economic activities. The model utilised in this work is based on the 2012 China input-output table (National Bureau of Statistic, 2015), which is the latest data of the Chinese economy. The details for the data source, data processing, model development and embodied emissions' computation could be found in the prior contribution (Li et al., 2019).

On the other hand, the process emissions reflect the direct environmental impacts, in which the pollutants caused by shale gas loss, consumptions of utilities, electricity are taken into consideration. The pollutants resulting from utilities, electricity and fired heat consumptions originate from their production. Relevant emissions are estimated according to the amount of required fuel gas and pollutant discharge coefficients.

4. Results and discussions

4.1 Economic evaluation of shale gas to methanol

The economic performance of the whole flowsheet is summarised in Figure 3(a). The dehydration process features the lowest values in both capital and operating costs. By contrast, the partial oxidation process has the highest capital cost, while methanol synthesis requires the highest operating cost. The TAC of shale gas to methanol is 12,235.3 k\$·y^{-1}. The distribution of capital cost for each process is depicted in Figure 3(b). In the dehydration process, the absorber and regenerator dominate the capital investment. The demethanizer accounts for 58.2 % of equipment cost in NGLs recovery system. In partial oxidation and methanol synthesis processes, the expenses of compressors take up about 50~60 % of ACC. The proportions of heat exchangers in ACCs are 14.7 % to 32.6 %. In terms of operating cost, the consumption of electricity is the dominant factor which accounts for 51.5 % of total AOP. This is because of the enormous demand for work in gas compression. The annual operating costs of hot utilities, cold utilities, fired heat and shale gas loss are 1,170.4 k\$·y^{-1}, 1,210.6 k\$·y^{-1}, 107.0 k\$·y^{-1} and 182.0 k\$·y^{-1}.
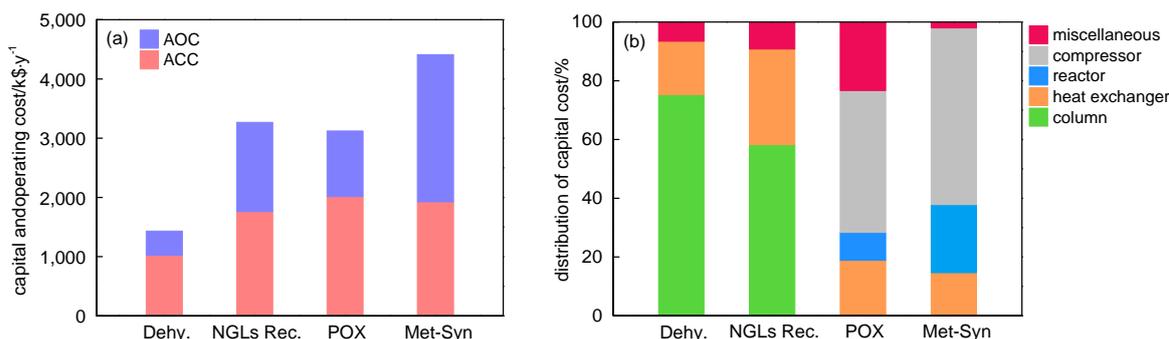
Figure 3: (a) Expenditure inventory of shale gas to methanol; (b) Distribution of capital cost in each process

4.2 Exergy analysis of shale gas to methanol

The exergy destruction in each process operation is summarised in Table 3. The POX reaction and methanol synthesis are dominant sources in exergy loss. The high temperature and pressure operating conditions might be one possible reason for effective energy loss. Moreover, the reactions also lead to massive chemical exergy destruction. As for heat exchanging, a larger heat transfer temperature difference brings about a greater irreversible loss, such as the cases in waste heat boiler and syngas/products cooling. The exergy loss from heat exchanging occupies 18.1 % of total amount. In addition, the valve in NGLs recovery system expands the dry gas and decreases its pressure to 3.2 MPa, leading to exergy destruction of 1,919.51 kW. In efforts to reduce exergy loss and save energy, it merits consideration to replace the valve with an expander.

Table3: Exergy destruction in each process

Process	item	Ex_d/kW
Dehydration	column	84.33
	heat exchanger	122.82
	pump	10.16
	miscellaneous	13.54
NGLs Recovery	column	426.93
	heat exchanger	2,020.88
	miscellaneous	2,210.38
Partial Oxidation	reactor	21,864.30
	heat exchanger	3,910.20
	compressor	277.74
	miscellaneous	3.48
Methanol Synthesis	reactor	9,750.64
	heat exchanger	1,732.72
	compressor	616.99
	miscellaneous	83.70
Total		43,128.81

4.3 Environmental assessment of shale gas to methanol

The environmental performance is evaluated by the hybrid LCI model. Figure 4 presents the impacts derived from each process by sources, in which the emissions of CO_2, SO_2, NO_x and soot are investigated. Dehydration process discharges the least pollutants owing to the minor usage in utilities and electricity. By contrast, methanol synthesis produces the largest amounts of pollutants, as a result of excess consumption of electricity. In terms of the whole process from shale gas to methanol, the annual emissions of CO_2, SO_2, NO_x and soot are 27,092.15 t/y, 33,667.26 kg/y, 48,496.81 kg/y and 9,499.01 kg/y.

As shown in Figure 4, electricity consumption is the predominant source of environmental impacts. It accounts for portions of 55.7 % in CO_2 emissions, 87.6 % in SO_2 emission and 77.7 % in NO_x emission. Since electricity is mainly generated from burning coals which is not a type of clean energy, the process that consumes much electricity reveals high discharge coefficient. That is the reason for the enormous pollutant emissions from methanol synthesis, which drives a compressor of 3,601.7 kW. Consequently, it is a promising approach to reduce environmental impacts by bringing in a work exchanger system to decrease the requirement of work.
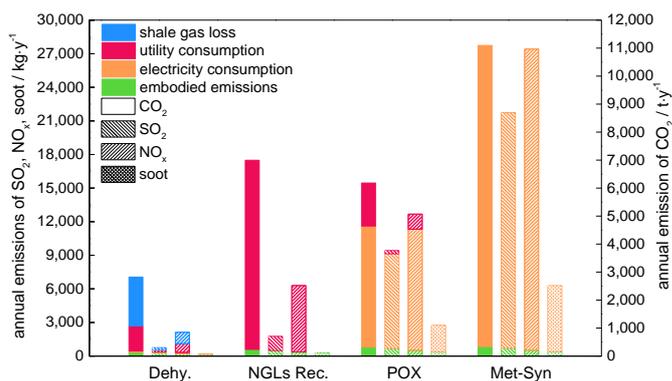
Figure 4: Environmental impacts derived from each process

5. Conclusions

In this study, the process of producing methanol from shale gas is simulated and investigated from economic, exergy and environmental perspectives. The economic target is estimated on the basis of the purchased cost curves, and the total annual cost of the whole process is 12,235.3 k$/y. The distribution of exergy destruction is obtained by exergy analysis. The reaction systems take up 73.3 % of total exergy loss. The environmental performance is assessed according to the hybrid LCI model. Annual emissions of CO_2, SO_2, NO_x and soot are investigated. The proposed model also indicates that electricity consumption is the dominant pollutant source. The methods in this study provide guidance for process design and environmental protection.

Acknowledgements

References

Aspen Technology Inc., 2014, Aspen Energy Analyzer user guide, Burlington, US.

Chang Y., Huang R.Z., Ries R.J., Masanet E., 2014, Shale-to-well Energy Use and Air Pollutant Emissions of Shale Gas Production in China, Applied Energy, 125, 147-157.

Ehlinger V.M., Gabriel K.J., Noureldin M.M.B., El-Halwagi M.M., 2014, Process Design and Integration of Shale Gas to Methanol, ACS Sustainable Chemistry & Engineering, 2(1), 30-37.

Energy Information Administration, 2013, Technically Recoverable Shale Oil and Shale Gas Resources: An Assessment of 137 Shale Formations in 41 Countries Outside the United States, Washington DC, US.

Julián-Durán L.M., Ortiz-Espinoza A.P., El-Halwagi M.M., Jimenez-Gutierrez A., 2014, Techno-Economic Assessment and Environmental Impact of Shale Gas Alternatives to Methanol, ACS Sustainable Chemistry & Engineering, 2(10), 2338-2344.

Kameyama H., Yoshida K., Yamauchi S., Fueki K., 1982, Evaluation of Reference Exergies for the Elements, Applied Energy, 11, 69-83.

Li W., Liu L., Zhang L., Meng Q., Du J., 2018, Optimization of Shale Gas Sweetening Process Coupling with Claus Process Based on Energy Synthesis, Chemical Engineering Transactions, 70, 1027-1032.

Li W., Zhuang Y., Liu L., Zhang L., Du J., 2019, Economic Evaluation and Environmental Assessment of Shale Gas Sweetening Process, Chemical Engineering & Technology, 42(4), 753-760.

National Bureau of Statistic, 2015, China Statistical Yearbook 2015, China Statistical Press, Beijing, China.

Ortiz-Espinoza A.P., Noureldin M.M.B., El-Halwagi M.M., Jimenez-Gutierrez A., 2017, Design, Simulation and Techno-economic Analysis of Two Processes for the Conversion of Shale Gas to Ethylene, Computers and Chemical Engineering, 107, 237-246.

Rahimi A.N., Mustafa M.F., Zaine M.Z., Ibrahim N., Ibrahim K.A., Hamid M.K.A., 2017, Optimal Retrofit of Natural Gas Liquids Separation Direct Sequence and Feed Condition Sensitivity Analysis, Chemical Engineering Transactions, 56, 1309-1314

Siirola J.J., 2014, The Impact of Shale Gas in the Chemical Industry, AIChE Journal, 60(3), 810-819.

Towler G.P. Sinnott R.K. 2013, Chemical Engineering Design: Principles, Practice, and Economics of Plant and Process Design, 2nd ed., Butterworth-Heinemann Elsevier Ltd., Oxford, UK.

Vanden Bussche K.M., Froment G.F., 1996, A Steady-State Kinetic Model for Methanol Synthesis and the Water Gas Shift Reaction on a Commercial Cu/ZnO/Al_2O_3 Catalyst, Journal of Catalysis, 161, 1-10.